

# Effect of Particle Size on Alkali-Activation of Slag

E. Petrakis, V. Karmali, K. Komnitsas

**Abstract**—In this study grinding experiments were performed in a laboratory ball mill using Polish ferronickel slag in order to study the effect of the particle size on alkali activation and the properties of the produced alkali activated materials (AAMs). In this regard, the particle size distribution and the specific surface area of the grinding products in relation to grinding time were assessed. The experimental results show that products with high compressive strength, e.g. higher than 60 MPa, can be produced when the slag median size decreased from 39.9  $\mu\text{m}$  to 11.9  $\mu\text{m}$ . Also, finer fractions are characterized by higher reactivity and result in the production of AAMs with lower porosity and better mechanical properties.

**Keywords**—Alkali activated materials, compressive strength, particle size distribution, slag.

## I. INTRODUCTION

METALLURGICAL industries generate very large amounts of slags that are considered as important sources of environmental pollution, if not properly recycled and utilized. Although considerable quantities are used in the construction sector, large volumes are still stockpiled and landfilled for long periods. From this point of view, the development of an integrated management scheme that can transform all these resources into valuable products is of great importance [1], [2].

Slags are mainly used for cement and concrete production. This utilization option eliminates environmental problems and contributes to the reduction of the environmental footprint of the construction sector. It is known that cement production is one of the most energy intensive processes, since it consumes 12 to 15% of the total industrial energy requirements and is responsible for 7 to 10% of the global CO<sub>2</sub> emissions [3], [4]. Other alternative options for slag management include its use in road construction as aggregate [5] and in recent years the production of AAMs, called inorganic polymers (IPs) or “geopolymers”, which can be used as construction materials or binders in the construction sector, thus improving its sustainability [6].

Alkaline activation, which is carried out with the use of NaOH, KOH and Na<sub>2</sub>SiO<sub>3</sub> solutions at relatively low temperature, is considered as a promising option for the management of various waste streams and the production of AAMs exhibiting beneficial physicochemical and thermal properties [7]-[10]. The potential of wastes for alkali activation depends on their content of aluminosilicates which

defines their reactivity, the strength of the activating solution and the other synthesis conditions, mainly particle size of the raw material used, curing temperature, curing and ageing period [11], [12].

Slag, prior to its use in most applications, requires grinding which is an energy intensive process, characterized by high CO<sub>2</sub> emissions and increased processing cost. In addition, grinding is a low-efficiency process because a large share of the consumed energy is absorbed by the device and only a small part is used for size reduction [13]. Considering these factors, the investigation of grinding kinetics of any raw material, including slag, is an important aspect.

The present study aims to evaluate the effect of grinding time on the particle size distribution of the slag products through batch grinding experiments. Then, selected grinding products were alkali activated and the effect of particle size on the properties of the produced AAMs was assessed.

## II. MATERIALS AND METHODS

The material used in this study is slag produced from the pyrometallurgical treatment of Ni-bearing silicate ores in Szklary, southwestern Poland [14]. The origin and the characteristics of this slag can be found in a previous recent study [2].

The received sample, approximately 200 kg, with particle size <100  $\mu\text{m}$  was homogenized by the cone and quarter method and a representative quantity was crushed to less than 0.850 mm using a jaw crusher for primary and a cone crusher for secondary crushing. The particle size distribution of the feed material and grinding products was determined using a Malvern type S Mastersizer (size range: 0.05 to 850  $\mu\text{m}$ ) and laser diffraction (LD) technique. The Brunauer-Emmett-Teller (BET) nitrogen adsorption method (using a Quantachrome Nova 2200 analyser) was considered for the determination of specific surface area (SSA) [15] of the products.

The techniques used for characterizing raw slag and the produced AAMs are (i) X-ray powder diffraction for the identification of the mineral phases using a D8 Advance type (Bruker-AXS) diffractometer and (ii) X-ray fluorescence for the chemical analysis using a Bruker S2 Ranger Energy-dispersive ED-XRF Spectrometer.

Grinding tests were carried out in a ball mill with dimensions of L x D = 166 x 204 mm using different grinding times (15, 30, 45, 60, 90 and 120 min) under dry conditions. Stainless steel balls ( $\rho_b = 7.85 \text{ g/cm}^3$ ) with three different sizes, i.e. 40, 25.4 and 12.7 mm were used as grinding media. The total ball mass was almost constant for each ball size used corresponding to ball filling volume  $J = 20\%$ , while the material filling volume  $f_c$  was 4%. This means that 50% of the interstitial filling  $U$  of the void spaces between the balls was

E. P. is with the School of Mineral Resources Engineering, Technical University of Crete, Kounoupidiana, 73100 Chania, Greece (corresponding author, phone: +30-28210-37608; fax: +30-28210-06901; e-mail: vpetraki@mred.tuc.gr).

V. K. and K. K. are with the School of Mineral Resources Engineering, Technical University of Crete, Kounoupidiana, 73100 Chania, Greece (e-mail: vkarmali@isc.tuc.gr, komni@mred.tuc.gr).

filled with material. The mill specification data and test conditions are shown in Table I.

TABLE I  
MILL SPECIFICATION DATA AND TEST CONDITIONS

mill	diameter, $D$ (cm)	20.4		
	length, $L$ (cm)	16.6		
	volume, $V$ (cm <sup>3</sup> )	5,423		
	operational speed, $N$ (rpm)	66		
	critical speed, $N_c$ (rpm)	93.7		
balls	diameter, $d$ (mm)	40	25.4	12.7
	number	6	28	202
	weight (g)	1572.7	1865.7	1702.4
	density (g/cm <sup>3</sup> )	7.85		
	porosity (%)	40		
	ball filling volume, $J$ (%)	20		
material	bulk density (g/cm <sup>3</sup> )	1.67		
	material filling volume, $f_c$ (%)	4		
	interstitial filling, $U$ (%)	50		

The grinding products obtained after 30, 60 and 120 min were alkali activated using a mixture of sodium hydroxide (NaOH, Sigma Aldrich) and sodium silicate (Na<sub>2</sub>SiO<sub>3</sub>, Merck) as alkaline activating solution. Pellets (anhydrous) of NaOH dissolved in water to produce solutions with specific molarity, followed by the addition of sodium silicate solution (8 wt% Na<sub>2</sub>O, 27 wt% SiO<sub>2</sub> and 65 wt% H<sub>2</sub>O). The final solution was allowed to cool at ambient temperature for 24 h and then mixed under continuous stirring with each grinding product to obtain a paste. Six sets of samples were prepared in order to investigate the effect of slag particle size and curing temperature (60 or 80 °C) on the produced AAMs while the liquid/solid (L/S) ratio was kept constant at 0.25. The composition of the mixture was (wt%): 80% slag, 16.7% 8 M NaOH solution and 3.3% Na<sub>2</sub>SiO<sub>3</sub>. Under these conditions the molar ratio of H<sub>2</sub>O/Na<sub>2</sub>O in the reactive paste was 12.9. The experimental procedure used is described in a recent study [2]. All tests and measurements were carried out in triplicate and average values are provided in this study. Finally, the apparent density, porosity and water absorption of selected AAMs was determined based on the standard BS EN 1936 [16].

### III. RESULTS AND DISCUSSION

#### A. Particle Size and SSA of Slag Products

The characteristic diameters of the cumulative distributions, i.e.  $d_{10}$ ,  $d_{50}$ ,  $d_{75}$  and  $d_{90}$ , which refer to particle sizes passing 10%, 50%, 75% or 90% cumulative undersize, were determined in order to investigate the fineness of the ground products obtained after different grinding times (Table II). This table also presents the SSA of the slag products determined by the BET technique. The results show that the characteristic diameters, also called equivalent particle sizes (EPSs), decrease during grinding and no agglomeration is observed as indicated by the  $d_{90}$  values (Table II) which continue to decrease during grinding. More specifically, the  $d_{90}$  of slag grinding product obtained after 15 min of grinding was 252.2  $\mu$ m and was reduced after prolonged grinding (120 min) to 47.1  $\mu$ m. Since surface area is intimately linked to

particle size, the results of Table II show that the SSA increases during grinding.

TABLE II  
EPS AND SSA OF SLAG GRINDING PRODUCTS AT DIFFERENT TIMES

Grinding time	BET	$d_{10}$	$d_{50}$	$d_{75}$	$d_{90}$
min	m <sup>2</sup> /kg	$\mu$ m	$\mu$ m	$\mu$ m	$\mu$ m
15	930	7.9	75.9	163.0	252.2
30	1200	4.2	39.9	88.8	153.8
45	1435	2.7	27.8	62.5	109.5
60	1598	2.1	23.4	51.8	86.2
90	2160	1.3	15.2	35.2	59.9
120	2260	1.0	11.9	28.1	47.1

#### B. Alkali-Activation of Slag

To investigate the effect of slag particle size on the compressive strength (CS) of the produced AAMs, three different median sizes ( $d_{50}$ ) of slag particles were selected, namely 39.9, 23.4 and 11.9  $\mu$ m which obtained after 30, 60 and 120 min of grinding, respectively. The other AAM synthesis conditions were 8 M NaOH, curing period 24 h and ageing period 7 days. Fig. 1 shows the CS of the AAMs produced as a function of particle size and curing temperature (60 or 80 °C). It is seen from the data that at 60 °C, when the median particle size of the raw material decreases from 39.9 to 11.9  $\mu$ m, the CS of the produced AAMs increases by 230%, from 7.9 to 26.2 MPa. On the other hand, when the curing temperature increases to 80 °C the produced AAMs obtain much higher CS which increases by 200%, from 20.2 MPa to 60.8 MPa, when the median particle size decreases from 39.9 to 11.9  $\mu$ m. These results indicate that when the raw material is finer and thus has larger surface area, the reactions with the activating solution proceed faster and thus the AAMs produced are denser and stronger.

Selected properties namely, apparent density (g/cm<sup>3</sup>), porosity (%) and water absorption (%) of the produced AAMs when different slag particle sizes were used are presented in Table III. This table also shows the CS of the AAMs produced under the conditions 8 M NaOH, curing temperature 80 °C, curing time 24 h and ageing period 7 days. It can be seen from the data that there is an evident difference in these properties of AAMs when three median sizes of slag particles were used. The main difference was observed in porosity which decreased from 13.5 to 6.7% when the slag median size decreased from 39.9 to 11.9  $\mu$ m, indicating that this property may have a significant influence on the CS of the produced AAMs. A similar trend was observed for water absorption which decreased from 5.9 to 3.8% by taking into account the same median sizes. On the other hand, the apparent density of the AAMs increased from 2.28 g/cm<sup>3</sup> when slag with median size 39.9  $\mu$ m was used to 2.54 g/cm<sup>3</sup> when the median size was 11.9  $\mu$ m.

The AAMs produced under the same synthesis conditions were also characterized with XRD, as seen in Fig. 2. The results indicate that the XRD patterns of the AAMs produced using different slag median size have no significant differences. The AAMs show a typical amorphous (broad hump between 20° and 40° 2 $\theta$ ) to semi-crystalline

composition consisting of several crystalline phases, i.e., quartz ( $\text{SiO}_2$ ), hedenbergite ( $\text{Ca}(\text{Fe,Mg})(\text{SiO}_3)_2$ ), fayalite ( $\text{Fe}_2\text{SiO}_4$ ), diopside ( $\text{CaMgSi}_2\text{O}_6$ ), magnetite ( $\text{Fe}_3\text{O}_4$ ) and hatrurite ( $\text{Ca}_3\text{SiO}_5$ ). It is noted that the XRD pattern of the raw slag does not show significant changes in terms of mineralogical composition. The results obtained also indicate that curing temperature is also an important parameter during alkali activation of slag. Increased curing temperatures accelerate alkali activating reactions and thus the produced AAMs exhibit better mechanical properties, as reported in previous studies [17], [18]. It is noted that the increase of ageing period from 7 to 28 days increases the CS slightly but the results are not provided in this study.

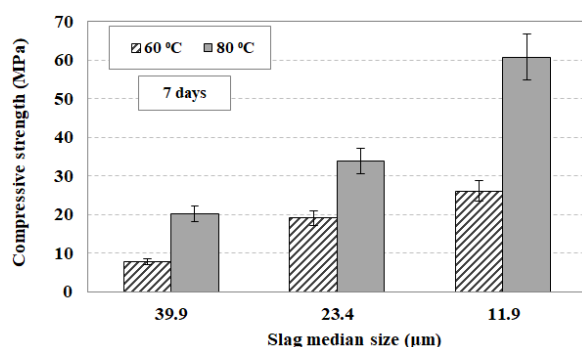


Fig. 1 Effect of slag median size as a function of curing temperature on the CS of the produced AAMs; synthesis conditions: 8 M NaOH solution, curing time 24 h, ageing period 7 days; median sizes of 39.9, 23.4, 11.9 μm derived after 30, 60, 120 min of grinding, respectively. Error bars indicate the standard deviation of three measurements

TABLE III  
SELECTED PROPERTIES OF AAMs PRODUCED UNDER THE CONDITIONS 8 M NaOH SOLUTION, CURING TEMPERATURE 80 °C, CURING TIME 24 H, AGEING PERIOD 7 DAYS

Slag median size	CS	Apparent density	Porosity	Water Absorption
μm	MPa	g/cm <sup>3</sup>	%	%
39.9	20.2	2.28	13.5	5.9
23.4	33.8	2.37	10.6	4.5
11.9	60.8	2.54	6.7	3.8

### C. Prediction of the CS of AAMs

Fig. 3 shows the effect of  $d_{50}$  slag particle size and BET SSA on the CS of the AAMs produced under the conditions 8 M NaOH, heating 80 °C, curing period 24 hours and ageing period 7 days. Three different median sizes of slag were used, namely 39.9, 23.4 and 11.9 μm. Table II shows the respective values of SSA of the slag grinding products. Simple regression analysis with the use of Excel software was carried out to establish potential correlations between CS and  $d_{50}$ , SSA and equations with the highest correlation coefficient  $R^2$  were obtained. As seen in Fig. 4, very strong correlation between CS and  $d_{50}$  is obtained using inverse exponential equation, while CS is correlated very well with SSA using linear equation. The experimental data were validated by additional experiments using as raw material slag with median size 15.2

μm (90 min of slag grinding) and the results are given in Fig. 4. It is noted that the use of slag with particle size obtained after 90 min of grinding results in the production of AAMs with a CS of 53.9 MPa. The obtained equations are:

$$CS = 660 \cdot d_{50}^{-0.95} \quad (1)$$

$$CS = 0.04 \cdot SSA - 30 \quad (2)$$

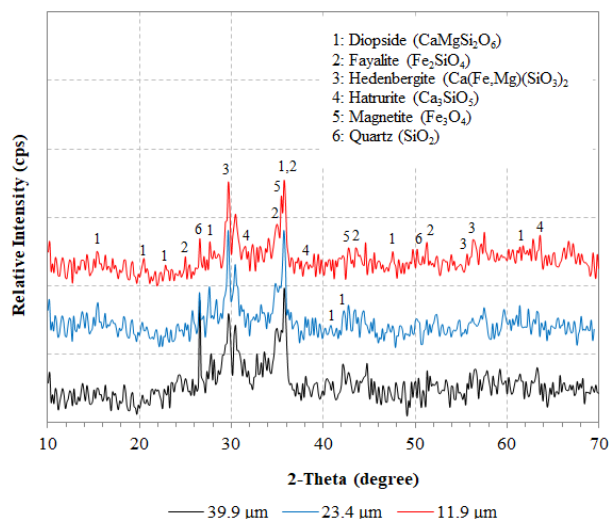


Fig. 2 XRD patterns of produced AAMs with different median sizes of slag particles were used. Synthesis conditions of AAMs were: 8 M NaOH solution, curing temperature 80 °C, curing time 24 h, ageing period 7 days

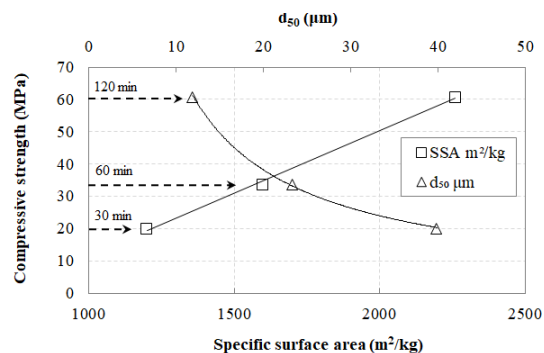


Fig. 3 Correlations between CS of AAMs produced and median size ( $d_{50}$ ), BET SSA of slag

Since particle size and SSA play a major role in the mechanical behavior of the obtained AAMs, these equations can be useful in predicting their CS.

### IV. CONCLUSION

The experimental results show that the particle size of slag products decreases with increasing grinding time and particle agglomeration is not observed even after prolonged grinding as indicated by the  $d_{90}$  values which continue to decrease during grinding.

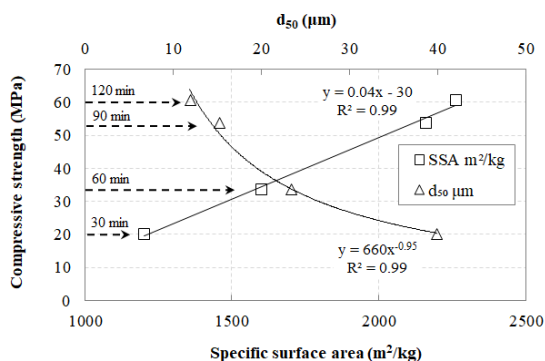


Fig. 4 Validation of the established correlations between CS of AAMs produced and median size ( $d_{50}$ ), BET SSA of slag

The results also indicate that the CS of the produced AAMs using selected fractions of raw slag is significantly affected by the slag particle size and SSA. The finer particles of the raw slag having larger surface area react faster with the activating solution and thus the produced AAMs exhibit higher CS. As a result, the maximum CS achieved was 60.8 MPa under the conditions 11.9  $\mu\text{m}$  slag median size, 8 M NaOH, curing temperature 80  $^{\circ}\text{C}$ , curing period 24 h and ageing period 7 days. The determination of selected properties of the produced AAMs revealed that porosity (%) and water absorption (%) decreased when the slag median size decreased, indicating that these properties may have a significant influence on the CS. As expected, the apparent density ( $\text{g}/\text{cm}^3$ ) showed an inverse trend. On the other hand, there were no significant differences in the XRD patterns of AAMs produced using different slag particle sizes. The results also indicate that curing temperature is a crucial parameter during alkali activation of raw materials. Increased curing temperature accelerates alkali activating reactions and thus AAMs with better mechanical properties are produced. In general, particle size and SSA of the raw material have a significant effect on the CS of the produced specimens and potential correlations between them can be established.

#### REFERENCES

- [1] L. Mo, F. Zhang, M. Deng, F. Jin, A. Al-Tabbaa, A. Wang, "Accelerated carbonation and performance of concrete made with steel slag as binding materials and aggregates," *Cem. Concr. Compos.*, vol. 83, pp. 138-145, 2017.
- [2] K. Komnitsas, G. Bartzas, V. Karmali, E. Petrakis, W. Kurylak, G. Pietek, J. Kanasiewicz, "Assessment of alkali activation potential of a Polish ferronickel slag," *Sustainability*, vol. 11, 1863, 2019.
- [3] C. Chen, G. Habert, Y. Bouzidi, A. Jullien, "Environmental impact of cement production: detail of the different processes and cement plant variability evaluation," *J. Clean. Prod.*, vol. 18, pp. 478-485, 2010.
- [4] M. Ali, R. Saidur, M. Hossain, "A review on emission analysis in cement industries," *Renew. Sust. Energ. Rev.*, vol. 15, pp. 2252-2261, 2011.
- [5] C. Maharaj, D. White, R. Maharaj, C. Morin, "Re-use of steel slag as an aggregate to asphaltic road pavement surface," *Cogent Eng.*, vol. 4, 1416889, 2017.
- [6] K. Komnitsas, "Potential of geopolymers technology towards green buildings and sustainable cities," *Procedia Eng.*, vol. 21, pp. 1023-1032, 2011.
- [7] A. Mehta, R. Siddique, "Sustainable geopolymer concrete using ground granulated blast furnace slag and rice husk ash: Strength and permeability properties," *J. Clean. Prod.*, vol. 205, pp. 49-57, 2018.
- [8] K. Komnitsas, D. Zaharaki, "Geopolymerisation: A review and prospects for the minerals industry," *Miner. Eng.*, vol. 20, pp. 1261-1277, 2007.
- [9] K. Komnitsas, D. Zaharaki, V. Perdikatsis, "Geopolymerisation of low calcium ferronickel slags," *J. Mater. Sci.*, vol. 42, pp. 3073-3082, 2007.
- [10] K. Komnitsas, D. Zaharaki, V. Perdikatsis, "Effect of synthesis parameters on the compressive strength of low-calcium ferronickel slag inorganic polymers," *J. Hazard. Mater.*, vol. 161, pp. 760-768, 2009.
- [11] H. Xu, J.S.J. Van Deventer, "The geopolymerisation of aluminosilicate minerals," *Int. J. Miner. Process.*, vol. 59, pp. 247-266, 2000.
- [12] D. Zaharaki, K. Komnitsas, V. Perdikatsis, "Use of analytical techniques for identification of inorganic polymer gel composition," *J. Mater. Sci.*, vol. 45, pp. 2715-2724, 2010.
- [13] E. Petrakis, E. Stamboliadis, K. Komnitsas, "Identification of optimal mill operating parameters during grinding of quartz with the use of population balance modelling," *KONA Powder Part. J.*, vol. 34, pp. 213-223, 2017.
- [14] J. Kierczak, C. Neel, J. Puziewicz, H. Bril, "The Mineralogy and weathering of slag produced by the smelting of lateritic Ni ores, Szklary, Southwestern Poland," *Can. Miner.*, vol. 47, pp. 557-572, 2009.
- [15] U. Kuila, M. Prasad, "Specific surface area and pore-size distribution in clays and shales," *Geophys. Prospect.*, vol. 61, pp. 341-362, 2012.
- [16] British Standards Institute. BS EN 1936: Natural Stone Test Methods. Determination of Real Density and Apparent Density and of Total and Open Porosity; NP EN 1936:2006; BSI: London, UK, 2007.
- [17] C.Y. Heah, H. Kamarudin, A.M. Mustafa Al Bakri, M. Binhussain, M. Luqman, I. Khairul Nizar, C.M. Ruzaidi, Y.M. Liew, "Effect of Curing Profile on Kaolin-based Geopolymers," *Phys. Procedia.*, vol. 22, pp. 305-311, 2011.
- [18] A. Soultana, A. Valouma, G. Bartzas, K. Komnitsas, "Properties of Inorganic Polymers Produced from Brick Waste and Metallurgical Slag," *Minerals*, vol. 9, 551, 2019.